

Mechanically Stretching Folded Nano- π -stacks Reveals Pico-Newton Attractive Forces

By Jung Sook Kim, Yu Jin Jung, Joon Won Park,* Andrew D. Shaller, Wei Wan, and Alexander D. Q. Li*

Hydrophobic attractions, such as aromatic π - π stacking, play an essential role in directing nanoscale molecular assembly, protein folding, DNA double-helix formation, host-guest recognition, and others.^[1–5] Proteins often activate hydrophobic interactions, to fold into unique structures in order to function properly, since misfolded proteins impair necessary functions, and sometimes cause certain diseases.^[6] Thus, understanding hydrophobic folding processes and their related behavior is critical. To better understand folding, reverse processes have been studied using cone-shaped dendrimers to further sharpen the atomic force microscopy (AFM) tip down to the molecular level. From the dendrimer apex, a highly specific single-strand DNA (ss-DNA) extends into solution ready to lock on to its complementary strand. The folded nano- π -stack ($N\pi S$) also contains two ss-DNA handles, one matching the dendrimer on the AFM tip and the other matching the dendrimer on the substrate, thus effectively bridging the AFM tip to a substrate; subsequent pulling of the AFM tip yields characteristic “nanospring”-like behavior at the single-molecule level.

AFM has become a powerful tool to study unfolding and refolding phenomena of nanostructured polymers, including synthetic foldamers (foldable polymers) and biological proteins.^[7–11] Single-molecule force spectroscopy, enabled by AFM, has offered novel perspectives, revealing structural and mechanical properties of biopolymers.^[12–19] Because one AFM tip typically has enough space to host several molecules, using available AFM tips to directly stretch a single molecule remains challenging. Dendron modification, however, sharpens the AFM tip down to the single-molecule level. Previously, self-assembled cone-shaped dendrons effectively spaced the reactive DNA molecules attached to the dendron apices. This controlled spacing removed lateral steric hindrance, enhanced hybridization efficiency and reproducibility, and greatly simplified the force-distance curve.^[20–24]

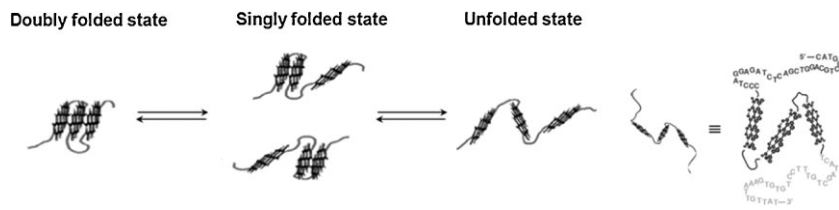
Obviously, an ss-DNA molecule ideally situated at the dendrimer apex can effectively hybridize to its complementary strand, providing the selectivity and specificity needed to fish out a desired target. Moreover, DNA hybridization offers tunable strength by varying the number of base pairs. Because DNA hybridizes reversibly, overwhelming AFM mechanical forces will not break the stretched macromolecule, but would rather unzip the DNA duplex; this enables repeated pulling of the same macromolecule.

As a model of folded domains, foldamers provide deep insight into folding intricacies because of their beautiful simplicity.^[25] The foldamer investigated here is a triblock polymer, DNA- $N\pi S$ -DNA, in which three perylene moieties form a thermophilic $N\pi S$, after actuating the flexible ethylene-glycol hinges (Scheme 1).^[26–28] Because the foldamer specifically hybridizes to the DNA molecules on the dendron-modified substrate and the AFM tip, it effectively bridges the AFM tip and the substrate. Hydrophobic effects strongly induce perylene moieties to fold into thermophilic nanostructures. Mechanical stretching, however, forces the doubly folded foldamer to adopt additional configurations—a singly folded state and an unfolded state—by repeated pulling. Highly reproducible elastic-folding behavior of the foldamer was observed with high precision.

The foldamer automatically locks on to the ss-DNA molecules on the AFM tip and the substrate when complementary DNA strands hybridize in a buffered solution. Cone-shaped dendrimers were briefly immobilized on both the AFM tip and a silicon wafer; their apices were functionalized with oligonucleotides (see Supporting Information). A 25-mer DNA whose sequence was complementary to the DNA at the 5'-end of the foldamer was attached to the AFM tip, while another 25-mer DNA whose sequence was complementary to the DNA at the 3'-end of the foldamer was bound to the substrate. After hybridizing the foldamer with the DNA on the substrate, the DNA-primed AFM tip approached the substrate, so that the second hybridization could occur. Retracting the AFM tip elongated the folded $N\pi S$, and eventually disengaged the substrate until DNA-DNA unzipping occurred. The observed perylene-peryene rupturing force was weaker than the DNA-DNA rupturing force (vide infra) and, consequently, perylene unfolding preceded the DNA-unzipping event while being pulled by the AFM tip. After rupturing of the DNA duplex, the foldamer could be positioned at either the silicon substrate or the AFM tip. When the AFM tip approached again, the complementary DNA hybridized again, reconnecting the substrate and the tip. This engagement enabled repeated force measurement in the retraction mode. Scheme 2 illustrates this process: the doubly folded state is being pulled to the singly folded state and then to unfolded states. Repeated

[*] Prof. J. W. Park, J. S. Kim, Dr. Y. J. Jung
Center for Integrated Molecular Systems
and Department of Chemistry
Pohang University of Science and Technology
San 31 Hyoja-dong, Pohang, 790-784 (Korea)
E-mail: jwpark@postech.ac.kr
Prof. A. D. Q. Li, A. D. Shaller, W. Wan
Department of Chemistry
and Center for Materials Research
Washington State University
Pullman, WA 99164 (USA)
E-mail: dequan@wsu.edu

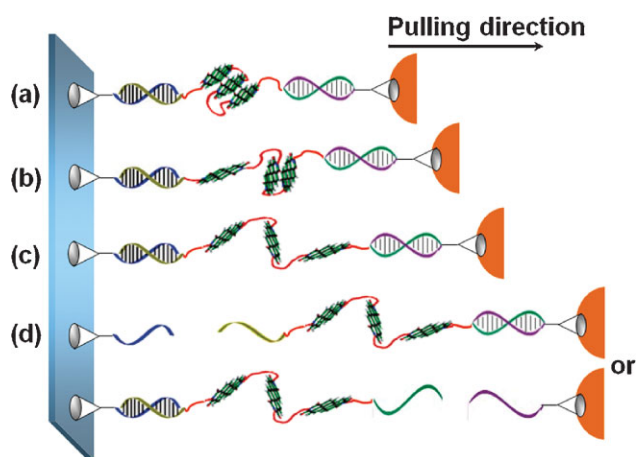
DOI: 10.1002/adma.200801323



Scheme 1. The AFM-stretched foldamer, a triblock polymer, has three domains: a folded chromophoric core ($N\pi S$) sandwiched by two DNA blocks. Its sequence is 5'-ssDNA- $N\pi S$ -ssDNA-3'. The $N\pi S$, consisting of $-(TEG-PDI-TEG)_3-$ (TEG: tetraethylene glycol; PDI: perylene tetracarboxylic diimide chromophore) can adopt a doubly folded state, a singly folded state, or an unfolded state, while being stretched.

pulling of the AFM tip using the foldamer on dendrons, complementary DNA without a $N\pi S$ on dendrons, and the foldamer without dendrons, revealed pico-Newton π - π stacking forces within the $N\pi S$.

With the foldamer on dendrons, repeated mechanical pulling yielded force–extension curves that exhibited reproducible small peaks before the last large peak. These small peaks had similar shapes and slopes, with critical characteristics that distinguished them from thermal noise, and were assigned to perylene–perylene unfolding or π -stack rupturing. The observed curves could be categorized into three types: a) curves with two consecutive small peaks and one large peak, b) curves displaying only one small peak and one large peak, and c) curves exhibiting only one large peak. Figure 1a–c shows typical force–extension curves obtained from the AFM pulling experiments. By repeating the AFM pulling experiment many times, the frequency of occurrence of each curve category was obtained. Type-a curves (doubly folded states) occurred in 34% (146/420) of the cases,



Scheme 2. The doubly folded foldamer is used to illustrate nonequilibrium mechanical unfolding. a) When the AFM tip approaches the surface, the far end of the foldamer (5') hybridizes with DNA bound to the AFM tip. b) As the AFM tip retracts upward, the first π -stack bursts. c) Further retraction induces the second perylene–perylene rupturing event. d) Finally, the DNA duplex gives up, and the foldamer may attach to either the substrate or the AFM tip; this completes the first pulling cycle. When the AFM tip approaches again, DNA hybridization again re-engages the tip with the substrate, and subsequent pulling reveals either the folded or unfolded states, depending on the refolding kinetics.

type-b curves (singly folded states) in 43% (179/420), and type-c curves (unfolded states) in 23% (95/420) of the cases. Figure 1d shows the distribution of the unfolding force during rupture of the $N\pi S$, and the force required to dislodge the DNA duplex at a loading rate of $0.54 \mu\text{m s}^{-1}$. The data indicate that the most probable unfolding force needed to actuate the perylene–perylene unfolding was 19 pN, and that needed to dislodge the DNA duplex was 35 pN. The histogram shapes and frequency distributions of the other curve categories closely resemble those displayed in Figure 1.

The $N\pi S$ -rupturing histograms overlap minimally with the DNA-rupturing histograms, suggesting that DNA–DNA unzipping does not occur before $N\pi S$ rupturing in most experiments.

To confirm the identity of the small peaks and the large peak, we replaced the $N\pi S$ with polyethylene glycol (PEG), and carried out identical pulling experiments. Instead of a foldamer, 5'-ssDNA-(PO_4 -TEG)- $_6$ -ssDNA-3' was used in this control experiment. Figure 2a displays a representative force–extension curve; the small peaks at 19 pN, which correspond to $N\pi S$ rupturing, disappeared, since the $N\pi S$ structure was removed from the macromolecular sequence. Additionally, the histogram of the rupture force reveals an average DNA–DNA dislodging force that agrees remarkably well with the light-gray histogram in Figure 1d. These results attribute the small peaks at ca. 19 pN to the $N\pi S$, and reconfirms that perylene–perylene rupturing yields these small peaks in Figures 1a and b.

The usage of dendrons effectively creates lateral spacing, separates each DNA-hybridization reaction, and practically enables the AFM tip to pull a single molecule at a time. In the second control experiment, the dendron was replaced by (3-aminopropyl)diethoxymethylsilane (APDES, see Supporting Information). The AFM tip and the substrate were treated with APDES in the same way as the dendron-modified surface before, being used to capture the foldamer for the stretching experiments. Repeated AFM pulling produced complex force–extension curves, sometimes containing a single peak, and most times containing multiple peaks (Fig. 2b). The occurrence of multiple peaks was prominent and overwhelming. While the force values from the last peak were incorporated to generate a histogram, the majority of the values were between 100 and 600 pN, an irregular distribution that could not be fit to a Gaussian function. The important corollary is that dendrons enabled the AFM tip to pull single foldamers, one at a time. The two control experiments confirm that the AFM tip is mostly pulling a single foldamer, and that the peaks at ca. 19 pN correspond to the perylene–perylene rupturing force.

Next, the effects of the loading speed and loading time were examined. A longer loading time allows more foldamers to return to equilibrium folded states, and yields more doubly and singly folded events; a faster loading rate captures the $N\pi S$ by surprise, and yields higher rupturing forces. To determine how the pulling velocity affected the perylene unfolding force, the forces were measured at velocities varying from 0.020 to $10 \mu\text{m s}^{-1}$. The force measured was plotted against the logarithm of the loading rate, $\ln r$. At the lowest speed, perylene–perylene unfolding was not

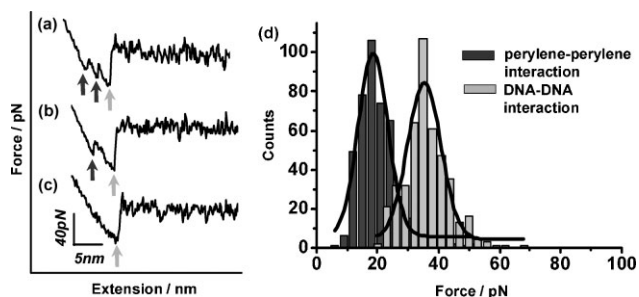


Figure 1. AFM pulling (at a loading rate of $0.54 \mu\text{m s}^{-1}$) induces π -stack unfolding and DNA-duplex bursting. The force–extension curves (a–c) and force histograms (d) clearly reveal the weak, noncovalent forces at pico-Newton levels. The dark-gray histogram and arrows correspond to the perylene attractive forces, while the light-gray histogram and arrows correspond to the DNA hybridization. Type-a curves exhibit two small peaks, type-b curves exhibit one small peak, and type-c curves exhibit no small peaks. d) Gaussian fitting gave the most probable rupturing forces of 19 and 35 pN for perylene and DNA, respectively.

discernible, because the extrapolated forces were ca. 10 pN, and were obscured by thermal noise. Figure 3 shows the observed linear relationship between the perylene unfolding force and $\ln r$. Such linearity suggests that the unfolding process experiences a single energy barrier in its energy landscape. If the unfolding path in the energy landscape has a single energy barrier, the most probable unbinding force, F , depends logarithmically on r , according to Equation 1 [29–31]

$$F = \frac{k_B T}{x_\beta} \ln \left(\frac{r x_\beta}{k_{\text{off}} k_B T} \right) \quad (1)$$

where T is temperature, k_B is the Boltzmann constant, x_β is a kinetic parameter known as the potential barrier length, and k_{off} is the kinetic off-rate constant or the dissociation constant. By fitting the data in Figure 3 to Equation 1, the two kinetic parameters, x_β and k_{off} , could be determined. Although no reference data are available to compare perylene–perylene interactions, dynamic

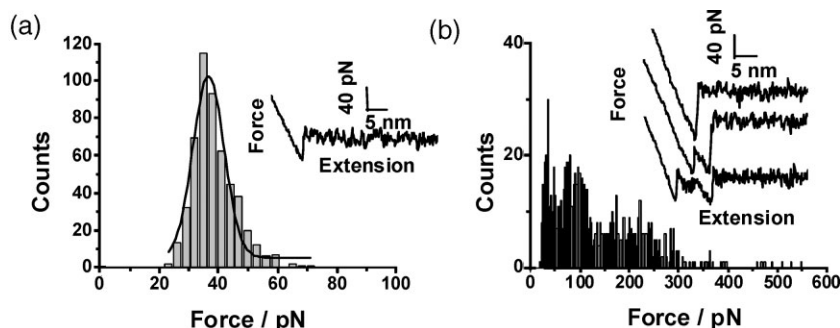


Figure 2. a) The control molecule without perylene moieties yields a histogram and a representative force–extension curve without peaks at 19 pN. The structure of the molecule is 5'-ssDNA-($\text{PO}_4\text{-TEG}$)₆-ssDNA-3', where the DNA sequence is identical to that of the foldamer. Gaussian fitting gave a most probable rupturing force of 37 ± 1 pN, similar to the DNA unzipping force observed in the foldamer. b) After replacing the dendrons on the substrate and the AFM tip with APDES, the measured force–extension curves became very complicated. The force values corresponding to the last peak were incorporated to generate the non-Gaussian histogram.

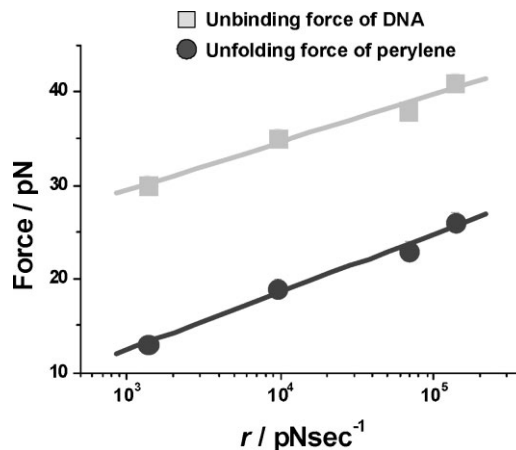


Figure 3. Both perylene–perylene unfolding forces (dark gray circles) and DNA-duplex unbinding forces (light-gray squares) depend on the AFM-tip pulling velocity. There is a good linear relationship between the pulling force and the logarithm of the loading rate for the unfolding $N\pi S$ yields.

force spectroscopy (DFS) studies on π -stack unfolding have yielded $x_\beta \approx 1.5$ nm and $k_{\text{off}} \approx 3.3 \text{ s}^{-1}$.

Finally, the effect of loading time on the frequency of occurrence of the three states was studied (see Supporting Information). Increasing the loading rate or reducing the loading time reduced the occurrence of both the doubly folded and singly folded states, presumably because the perylene unit did not have sufficient time to refold at such fast pulling speeds. The optimum speed with which to observe doubly folded states seemed to be $0.54 \mu\text{m s}^{-1}$. The AFM pulling forces overwhelmed the weak secondary molecular interactions; such nonequilibrium processes might have rendered foldamers into either trapped states or large-entropy states, which were slow to return to equilibrium. Nonetheless, some interesting kinetic data were observed when the foldamers did return to the folded states within the cycle period of 1.7 s, although the amenable range was relatively narrow.

To conclude, single-molecule unfolding behavior associated with foldamers was observed, and the nonequilibrium doubly folded, singly folded, and unfolded states were statistically quantified. The analysis revealed the presence of a single energy barrier during rupture of the $N\pi S$. The employed loading rate was sufficient to allow considerable foldamers to return to the folded or partially folded states.

Experimental

Sample Preparation: DNA-functionalized dendrons were immobilized on the silicon substrate and AFM probe as previously described (see Scheme S1a, Supporting Information) [24]. After modifying the silicon substrate and AFM probe, the foldamer solution (100 nm in phosphate buffered saline (PBS) buffer (pH 7.4)) was placed on the complementary DNA-primed substrates to initiate the hybridization reaction. The substrates were incubated at 55°C for 1 h, and rinsed thoroughly with PBS buffer to remove nonspecifically bound foldamer. After

washing, the substrates were used immediately for the AFM measurements. In the first control experiment, a molecule with an identical structure, aside from the perylene moieties, was examined under the same experimental conditions. In the second control experiment, the substrate and the AFM tip were silylated with APDES, to demonstrate the effectiveness of the dendron modification.

AFM Force Measurement: AFM force measurements were performed using a NanoWizard AFM microscope (JPK Instrument). The spring constant of each AFM tip was calibrated using the thermal fluctuation method right before each experiment. Each AFM probe had a characteristic spring constant, ranging from 13 to 17 pN nm⁻¹. The deflection from the lowest point of a peak to the baseline in the force–extension curves was converted to the unbinding force by applying the spring constant. The baseline bisected the thermal noise, and was parallel to the x-axis. All measurements were carried out in a fresh PBS buffer (pH 7.4) with a fluid cell at 25 °C (JPK Instrument). For the analysis, the force curves were recorded at a given position until the DNA–DNA unbinding curves could not be obtained successfully and continuously. Typically, the tip was moved to a new position after measuring the force–extension curves approximately one hundred times, and the curves were recorded at six to 10 positions.

Acknowledgements

J.W.P. acknowledges the Center for Integrated Molecular Systems (KOSEF), the Next Generation New Technology Development Program (MOCIE), the Nano/Bio Science & Technology Program of MOST (2008-00759), and Brain Korea 21. A.D.Q.L. acknowledges the National Institute of General Medicine Sciences (Grant GM065306). A.D.Q.L. was a Beckman Young Investigator (BYI). Supporting Information is available online from Wiley InterScience or from the author.

Received: May 14, 2008

Revised: August 1, 2008

Published online:

- [1] M. L. Waters, *Curr. Opin. Chem. Biol.* **2002**, *6*, 736.
- [2] E. A. Meyer, R. K. Castellano, F. Diederich, *Angew. Chem. Int. Ed.* **2003**, *42*, 1210.
- [3] A. Rich, A. Nordheim, A. H. J. Wang, *Annu. Rev. Biochem.* **1984**, *53*, 791.
- [4] D. A. Britz, A. N. Khlobystov, *Chem. Soc. Rev.* **2006**, *35*, 637.
- [5] S. Woo, Y. Lee, V. Sunkara, R. K. Cheedarala, H. S. Shin, H. C. Choi, J. W. Park, *Langmuir* **2007**, *23*, 11373.
- [6] N. Gregersen, P. Bross, S. Vang, J. H. Christensen, *Annu. Rev. Genomics Hum. Genet.* **2006**, *7*, 103.
- [7] H. Clausen-Schaumann, M. Seitz, R. Krautbauer, H. E. Gaub, *Curr. Opin. Chem. Biol.* **2000**, *4*, 524.
- [8] T. E. Fisher, P. E. Marszalek, J. M. Fernandez, *Nat. Struct. Mol. Biol.* **2000**, *7*, 719.
- [9] G. Hummer, A. Szabo, *Acc. Chem. Res.* **2005**, *38*, 504.
- [10] S. Yamamoto, Y. Tsujii, T. Fukuda, *Macromolecules* **2000**, *33*, 5995.
- [11] W. Zhang, X. Zhang, *Prog. Polym. Sci.* **2003**, *28*, 1271.
- [12] M. Rief, M. Gautel, F. Oesterhelt, J. M. Fernandez, H. E. Gaub, *Science* **1997**, *276*, 1109.
- [13] P. E. Marszalek, H. Lu, H. Li, M. Carrion-Vazquez, A. F. Oberhauser, K. Schulten, J. M. Fernandez, *Nature* **1999**, *402*, 100.
- [14] P. M. Williams, S. B. Fowler, R. B. Best, J. L. Toca-Herrera, K. A. Scott, A. Steward, J. Clarke, *Nature* **2003**, *422*, 446.
- [15] H. Dietz, M. Rief, *Proc. Natl. Acad. Sci. USA* **2004**, *101*, 16192.
- [16] M. Kessler, H. E. Gaub, *Structure* **2006**, *14*, 521.
- [17] J. R. Forman, J. Clarke, *Curr. Opin. Struct. Biol.* **2007**, *17*, 58.
- [18] A. F. Oberhauser, P. E. Marszalek, M. Carrion-Vazquez, J. M. Fernandez, *Nat. Struct. Mol. Biol.* **1999**, *6*, 1025.
- [19] C. McAllister, M. A. Karymov, Y. Kawano, A. Y. Lushnikov, A. Mikheikin, V. N. Uversky, Y. L. Lyubchenko, *J. Mol. Biol.* **2005**, *354*, 1028.
- [20] B. J. Hong, S. J. Oh, T. O. Youn, S. H. Kwon, J. W. Park, *Langmuir* **2005**, *21*, 4257.
- [21] B. J. Hong, J. Y. Shim, S. J. Oh, J. W. Park, *Langmuir* **2003**, *19*, 2357.
- [22] B. J. Hong, V. Sunkara, J. W. Park, *Nucleic Acids Res.* **2005**, *33*, e106.
- [23] S. J. Oh, J. Ju, B. C. Kim, E. Ko, B. J. Hong, J.-G. Park, J. W. Park, K. Y. Choi, *Nucleic Acids Res.* **2005**, *33*, e90.
- [24] Y. J. Jung, B. J. Hong, W. Zhang, S. J. B. Tandler, P. M. Williams, S. Allen, J. W. Park, *J. Am. Chem. Soc.* **2007**, *129*, 9349.
- [25] J. J. Han, W. Wang, A. D. Q. Li, *J. Am. Chem. Soc.* **2006**, *128*, 672.
- [26] W. Wang, J. J. Han, L.-Q. Wang, L.-S. Li, W. J. Shaw, A. D. Q. Li, *Nano Lett.* **2003**, *3*, 455.
- [27] W. Wang, L.-S. Li, G. Helms, H.-H. Zhou, A. D. Q. Li, *J. Am. Chem. Soc.* **2003**, *125*, 1120.
- [28] W. Wang, W. Wan, H.-H. Zhou, S. Niu, A. D. Q. Li, *J. Am. Chem. Soc.* **2003**, *125*, 5248.
- [29] R. Merkel, P. Nassoy, A. Leung, K. Ritchie, E. Evans, *Nature* **1999**, *397*, 50.
- [30] T. Strunz, K. Oroszlan, R. Schäfer, H.-J. Güntherodt, *Proc. Natl. Acad. Sci. USA* **1999**, *96*, 11277.
- [31] R. Eckel, S. D. Wilking, A. Becker, N. Sewald, R. Ros, D. Anselmetti, *Angew. Chem. Int. Ed.* **2005**, *44*, 3921.